Journal of Computers Vol. 34 No. 4, August 2023, pp. 175-183
doi: 10.53106/199115992023083404015

Machine Vision Based Defect Detection Method for Electronic Component Solder Pads

Xiaoning Bo[1,2*], Jin Wang[1], Honglan Li[1], Guoqin Li[1], Feng Lu[1]

[1] Department of Electrical Engineering, Taiyuan Institute of Technology, Taiyuan 030008, China
[2] School of Information and Communication Engineering, North University of China, Taiyuan 030051, China
boxn@tit.edu.cn, wangj@tit.edu.cn, lihonglan0207@126.com,
ligq@tit.edu.cn, lufeng@tit.edu.cn

Received 1 July 2023; Revised 20 July 2023; Accepted 25 July 2023

Abstract. This paper proposes a machine vision based solder pad detection method to improve the detection accuracy and efficiency of PCB solder pad defects in electronic components due to missed detection and low detection efficiency. Firstly, preprocess the electronic component pad images collected by the visual system, then use threshold segmentation method to perform preliminary segmentation of the pad images. Then, the coarse segmented images are finely segmented using mean clustering method, and the fine segmented images are pixel edge extracted. Finally, the matrix subpixel edge detection method is used to improve the edge detection accuracy. Simulation experiments have shown that the proposed method can significantly improve the accuracy and speed of defect recognition.

Keywords: machine vision, pad, deep learning, Faster R-CNN

1 Introduction

With the development of intensive and refined electronic circuits, as well as the characteristics of multiple pins, small spacing, and high welding accuracy requirements of chips and SMT components, the accuracy and stability of the detection results using manual magnifying glass or microscope visual inspection methods cannot meet the needs of modern automated production.

The development of computer vision technology has provided ideas for automated recognition and detection. Micro welding scenes such as chip pads and component pins can be processed with high clarity through machine vision. In addition, with the development of automatic recognition algorithms and artificial intelligence technology, the automatic recognition and defect diagnosis technology of pin welding continuously improves the efficiency and yield of chip welding production.

However, with the miniaturization of electronic components, it brings higher challenges to the production process of electronic circuits. This article takes the PCB pad of electronic components as the research object, and studies common defect detection methods such as pad solder failure, solder accumulation, and pinching. To improve the defect detection ability of solder pads, the work done in this article is as follows:

1) Firstly, the solder pad image of electronic components is processed and the processing process is described, including coarse segmentation, fine segmentation, and pixel edge extraction of the image.

2) The processed images are fed into the network recognition channel, and the network structure is improved based on Faster R-CNN. The improvement mainly focuses on the RPN module. The improved network can avoid falling into local optima, while improving recognition speed and accuracy.

In order to fully describe the method of this article, the chapters are arranged as follows: Chapter 2 mainly introduces the relevant research status, Chapter 3 mainly describes the processing and segmentation process of fine images, Chapter 4 mainly introduces the improvement process of deep learning algorithms, and provides improvement results. The final chapter is the conclusion section.

* Corresponding Author

2 Related Work

Wenjing Li proposed a pin welding defect detection method based on machine vision, which uses image enhancement, image filtering, threshold segmentation, and morphological processing algorithms to achieve accurate detection of defects in images [1]. Kai Zeng used the YOLOv3-SSD object detection algorithm to construct a welding defect detection model. Then, he used techniques such as model pruning, model distillation, and model quantization to compress and optimize the detection model, ultimately achieving fast and accurate recognition of welding defects and positioning of defect positions, solving the problems of low efficiency and high rate of missed and false detections caused by manual visual inspection [2]. Zhipeng Liu collected images from industrial cameras for packaging pads and selected qualified PCB bare board images as templates; Collecting bare PCB board images for testing, performing coarse and fine segmentation processing, etc. The results show that the detection speed and reliability have been improved [3]. Zhisheng Dai used a visual based method to automatically identify solder balls, pin bridges, missing solder joints, and qualified situations at the patch pins, and solved the adaptability problem for different light intensities, improving the accuracy of identifying pin welding defects [4]. Wei Liang used X-ray method to collect two-dimensional images of solder pads, then used time domain sequence image integration method to reduce image noise, enhance details, and finally used extreme point search algorithm to determine the size and location of defects. The experimental results proved the improvement of detection accuracy [5].

3 Localization and Feature Extraction of Solder Pad Pin Area

The entire recognition framework for visually based defect detection of electronic component backboard solder pads consists of an image acquisition system, motion control system, and image processing system. The system schematic is shown in Fig. 1.

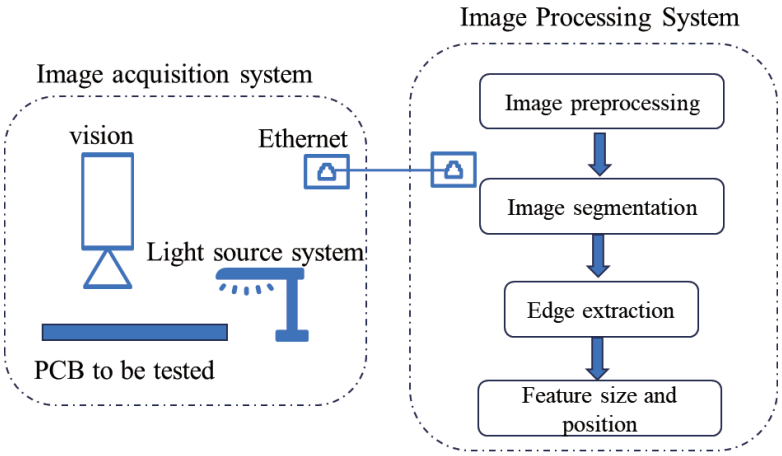

Fig. 1. System schematic diagram

The system schematic experiment uses a 10 megapixel industrial camera to collect images of electronic component backboard pads. The images are transmitted to the image processing system through a USB cable. The image processing system analyzes and recognizes the incoming images, and uses a series of image preprocessing methods to locate the center of the solder joint area [6]. After rotation transformation, the extracted pin center area is shown in Fig. 2.

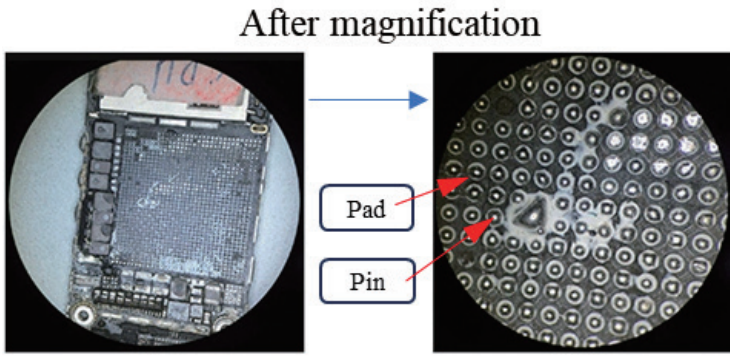

Fig. 2. Physical diagram of electronic component welding

3.1 Pin Pad Detection Algorithm

Algorithm description: In response to the uneven design of the pins in this patch, which results in discontinuous connected domains after binarization of the pins, this article proposes a global and local approach. Firstly, the binary image of the pin area is filtered for connected domains, and then the image is divided into two parts. Firstly, the right half of the lead area (right area) is identified. If the detection result is defective, the detection result is directly determined; If the right area is qualified, the overall area needs to be identified, and the algorithm process is shown in Fig. 3.

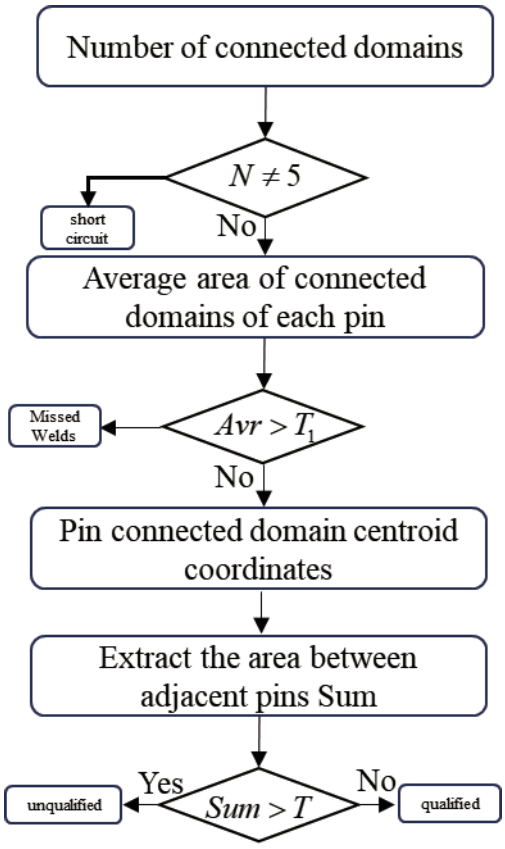

Fig. 3. Flow chart for identifying pin welding defects

3.2 Image Processing

After graying out the extracted pin area image, the maximum inter class difference method is used for threshold segmentation. Due to the influence of noise and flux reflection effect, there are some small connected domains in the binarized image, which interfere with pin welding defect detection. This article marks the connected domains in the binarized image and uses the connected domain area filtering method to filter out connected domains with an area smaller than the threshold T, Set the value of its corresponding position to 0 and preserve the connected domain with an area greater than the threshold T. Due to the fact that the pins of this SMD component are not straight and there is a certain height difference on the PCB plane, the incompleteness of the pin connected domain occurs after the threshold segmentation of the pin region. The filtered effect is shown in Fig. 4.

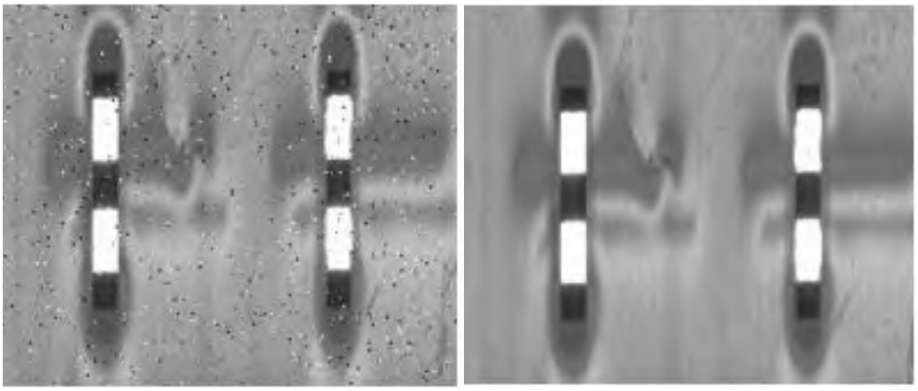

Fig. 4. Image filtering processing results

3.3 Image Segmentation

Calculate the gray-scale histogram of PCB pad image, set the gray-scale threshold range as [6, 43] according to the gray-scale histogram, and perform binary processing on the Grayscale of PCB pad. If the gray-scale value of (x, y) at any point on it is $f(x, y)$, and set the processed image as D, then it is expressed as:

$$g(x,y)=\begin{cases}1 & f(x,y)>T\\ 0 & f(x,y)\le T\end{cases}. \tag{1}$$

The coarse segmentation effect is shown in Fig. 5.

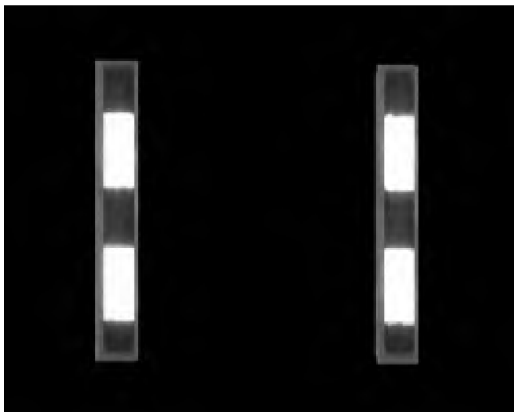

Fig. 5. Coarse segmentation rendering

Due to environmental factors such as lighting, it is difficult to determine an appropriate threshold using threshold segmentation method, and the segmentation effect of PCB pads is not very ideal. In order to more accurately extract the edge information of PCB pads, based on the pixel grayscale features of the image, an improved K-mean algorithm is used to finely segment the coarse segmented area of PCB pad images into pad areas and background areas [7]. The coarse segmented area pixels of the pad image are initialized, and after rough segmentation, the clustering center point of the image has been preliminarily determined. Therefore, in the clustering process, data as far away as possible is selected as the clustering center. The steps are as follows:

Input: K, the number of cluster clusters, and set to 3;

D. A dataset containing n objects, this article assumes $n = 5$;

Output: Set of K clusters and class number $\{D_1, D_2, D_3\}$;

Cluster target setting: minimize the sum of squares of various errors.

$$f_{SSE} = \sum_{j=1}^{k} \sum_{p \in D_j} \left\| p - n_j \right\|^2 . \tag{2}$$

In the formula, D_j is the j -th cluster, p is the sample point in D_j, n_j is the cluster center of D_j, which is the mean of all samples in D_j, and f_{SSE} is the clustering error of all samples, representing the quality of clustering performance.

The clustering center should satisfy the following relationship:

$$\frac{\partial f_{SSE}}{\partial n_j} = \frac{\partial}{\partial m_j} \left[\sum_{j=1}^{k} \sum_{p \in D_j} (p - n_j)^2 \right] = \sum_{j=1}^{k} \sum_{p \in D_j} \frac{\partial}{\partial n_j} \left(p - n_j \right)^2 = \sum_{p \in D_j} 2 \left(p - n_j \right) = 0. \tag{3}$$

Randomly select one sample from $\{D_1, D_2, D_3\}$ as the initial clustering center, calculate the distance between the three samples and the nearest clustering center, set it as $L(X)$. Select new data as the clustering center, and the probability of selection is proportional to $L(X)$. Until all the clustering centers are selected and the iteration ends, otherwise continue the iteration.

3.4 Pixel Precision Edge Extraction

Using the fitting method to detect pixel edges, first establish a grayscale model of the edge, and then fit according to the minimum distance between each grayscale value and the fitting curve. First, calculate the gradient of the image to extract the edge [8]. Considering the symmetry of expansion and corrosion operations, use the basic gradient to obtain pixel level edges. The mathematical expression is:

$$\nabla I(x, y) = \left[\frac{\partial I(x, y)}{\partial x}, \frac{\partial I(x, y)}{\partial y} \right] = \left[I_x, I_y \right]. \tag{4}$$

The size of the gradient is expressed as:

$$\left\| \nabla I(x, y) \right\| = \sqrt{I_x^2 + I_y^2} . \tag{5}$$

The gradient direction is expressed as:

$$a(x, y) = \arctan \frac{I_x}{I_y}. \tag{6}$$

In the formula, $I(x, y)$ represents the grayscale value of the original image, $\nabla I(x, y)$ represents the pixel gradient, and the amplitude of the maximum gradient direction is $\| \nabla I(x, y) \|$. Use Gaussian fitting to obtain sub-pixel coordinates. Since the Gaussian function curve is monotonically increasing on the left side of the symmetry axis, pixel grayscale should be increasing and decreasing on both sides of the pixel level edge. Digital images are

essentially a two-dimensional discrete grayscale matrix, and in order to obtain the subpixel positions of edges, a continuous grayscale mathematical model must be established. The edge of this image is not an ideal stepped edge. It is generally believed that the actual edge is formed by convolution of a step edge and a Gaussian function. Without considering the influence of noise, its mathematical model can be expressed as:

$$g(x) = T \times \exp\left(-\frac{(x - x_0)^2}{2 \times \delta^2} \right). \tag{7}$$

In the formula, $g(x)$ is the grayscale value when the pixel coordinate is x, T is the maximum pixel value, δ is the standard deviation, and x_0 is the mean. Each value is solved through fitting. Calculate the Natural logarithm of the Gaussian function and get:

$$G(x) = \ln g(x). \tag{8}$$

Formula transformation yields:

$$G(x) = \ln A - \frac{x_0}{2 \times \delta^2} + \frac{x_i \times x_0}{\delta^2} - \frac{x_i^2}{2 \times \delta^2}. \tag{9}$$

The theoretical pixel gray level $G_i = \{G_1, G_2, ..., G_n\}$ can be obtained by bringing the pixel coordinate into formula 9. The purpose of fitting is to minimize the difference between the theoretical pixel gray level and the actual pixel gray level. Use the least square method to fit the curve, and calculate the Partial derivative of the sample center points d_1, d_2, d_3, and finally obtain the following formula:

$$\begin{bmatrix} d_1 \\ d_2 \\ d_3 \end{bmatrix} = \begin{bmatrix} n & \sum x_i & \sum x_i^2 \\ \sum x_i & \sum x_i^2 & \sum x_i^3 \\ \sum x_i^2 & \sum x_i^3 & \sum x_i^4 \end{bmatrix}^{-1} \begin{bmatrix} \sum G(x_i) \\ \sum x_i G(x_i) \\ \sum x_i^2 F(x_i) \end{bmatrix}. \tag{10}$$

Substitute the obtained d_1, d_2, and d_3 into formula 7 to obtain the pixel edge position and complete edge extraction.

4 Deep Learning Algorithm for Defect Recognition

The processed image information is fed into a deep learning model, which automatically recognizes defect features. This article builds a recognition model based on Faster RCNN network and optimizes and improves it. The model consists of two parts: RPN and Faster RCNN. RPN is responsible for generating high-quality region suggestions, while Faster RCNN is responsible for classifying and regressing regions [9].

Select ResNet-15 with more network layers to replace the VGG16 network in the original network. Deeper ResNet-15 networks can learn shallow information and have stronger feature extraction capabilities for small target objects. However, the increase in network depth can also cause the output dimension to become larger, leading to an increase in the overall computational load of the structure, slowing down the detection speed. Three convolutional kernels of different sizes are used for convolution and maximum pooling operations, increasing module width, reducing parameter computation, and finally connecting each output stage as the total output, improving the detection speed.

Since the pads detected in this paper are tiny feature information, after the image passes through the Activation function, it is first processed by 3×3 -convolution to reduce the dimension, then a 5×5 -convolution is decomposed into two 3×3 -convolutions to expand the Receptive field of the network, but the calculation amount is reduced by a quarter, and finally the channel is normalized by D-convolution. The improved Faster RCNN network structure is shown in Fig. 6.

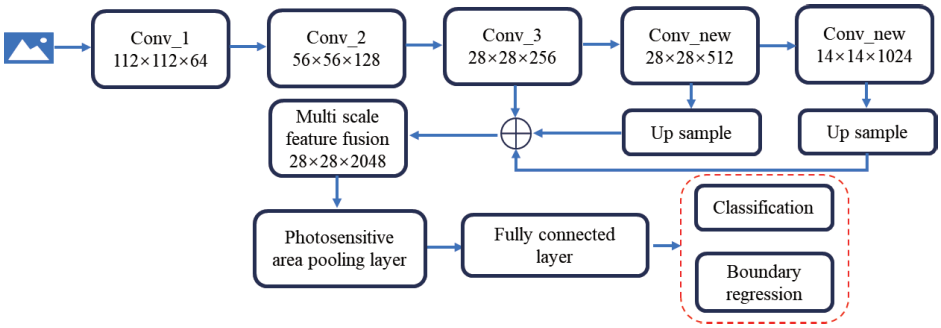

Fig. 6. Improved network structure diagram

5 Simulation Experiment and Analysis

5.1 Dataset Production

Collect electronic component solder pad defect images through a real working environment. The defect images mainly include three common defects: false soldering, excessive solder, and pinching. A total of 200 images were collected, and the images were expanded to 800 through flipping, color processing, and other methods. The proportion was controlled in the images. Due to the higher probability of excessive stacking and false soldering in practice, the ratio was 3:3:2 in the dataset, which means 300 false soldering and 300 solder excess, Pull 200 pieces., Manually annotate 800 solder pad defect images using Labelme standard software to obtain JSON files of defect locations and types in the defect images; Then convert its format into an XML file; Finally, divide the training and testing sets of the solder pad defect dataset, randomly allocate 600 cigarette label defect images to the training set and 200 images to the testing set. The defect markings are shown in Fig. 7.

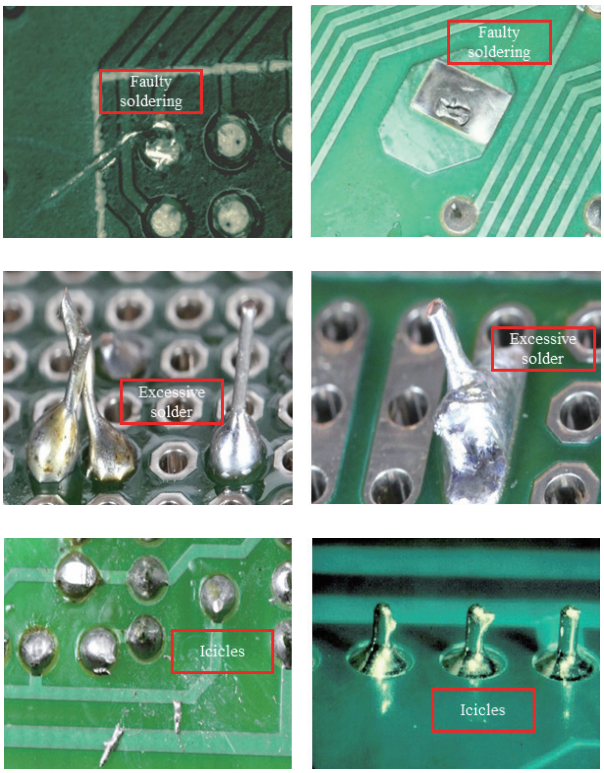

Fig. 7. Defect marking

5.2 Model Parameter Settings

The experimental software environment for this article is Windows 10; The hardware environment is an Intel CORE i7-9700K processor, with 32GB of memory and NVIDIA RTX2060S 8G independent graphics card; The development environment is CUDA10.1 and OPENCV3.4.2. Train and test the model using the Py - torch deep learning framework. This article selects Yolov4, SSD, and Faster R-CNN as the comparison algorithms before improvement. The recognition accuracy and recognition speed of each algorithm are compared through dataset validation. The comparison results are shown in Fig. 8.

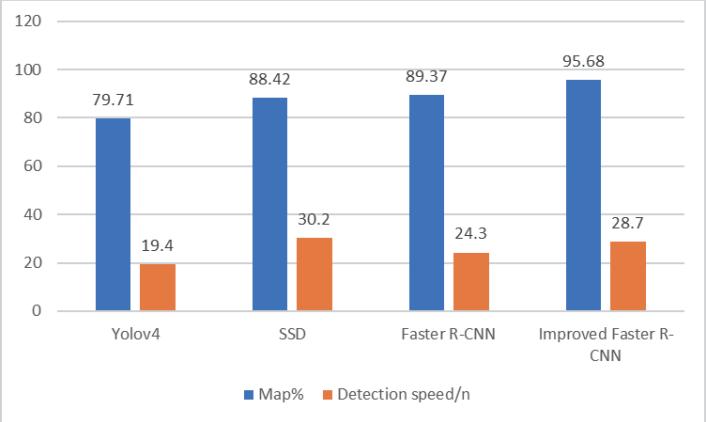

Fig. 8. Algorithm comparison results

The model inspection results show that the SSD model has the fastest detection speed for welding defects, and the improved Faster R-CNN has the highest accuracy for welding defects. YOLOV4 and SSD have similar detection speeds for welding defects, but the detection accuracy is relatively low, not exceeding 90%. The improved Faster R-CNN has a 6.31% increase in accuracy compared to the improved Faster R-CNN. Although SSD has a faster detection speed compared to the improved Faster R-CNN, due to the high precision requirements for welding defect detection, the improved Faster R-CNN is more suitable for welding defect detection.

5.3 Detection Result

In order to better validate the effectiveness of the algorithm in this article, three defect photos were selected for recognition analysis, and the analysis results are shown in Fig. 9. After experiments, the recognition accuracy of each defect has reached the expected level, but it can also be seen from the results that the recognition ability for the pull tip needs to be improved. The reason for this is also largely related to the lack of training images.

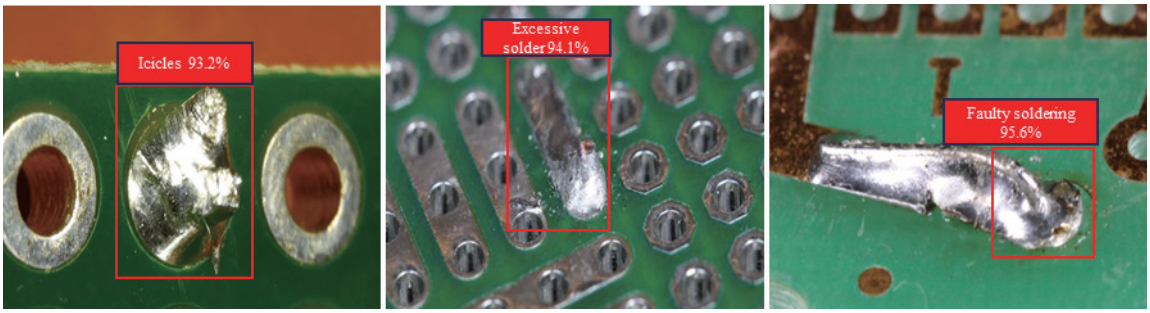

Fig. 9. Recognition result

6 Conclusion

This article improves image processing methods and network structure to achieve recognition of solder pad pin defects, while achieving high recognition accuracy and speed. Further research will mainly focus on the dataset of defect images and the training of models, continuously improving the recognition ability of the models.

Acknowledgement

This work has been supported by Scientific and Technologial Innovation Programs of Higher Education Institutions in Shanxi Province (2022L533, 2022L534).

References

[1] W.-J. Li, H.-S. Zhang, J. Jiao, Welding Defect Detection Algorithm for Chip IC Based on HALCON, Journal of Ordnance Equipment Engineering 41(8)(2020) 244-248.
[2] K. Zeng, X. Li, J.-M. Jia, J.-F. Wen, X. Wang, Optimal Model for Defect Detection Based on YOLOv3-spp, Computer Systems & Applications 31(2)(2022) 213-219.
[3] Z.-P. Liu, Q.-Z. Zhang, Y.-L. Zhou, Defect detection of BGA pads based on machine vision, Journal of Beijing Information Science & Technology University 31(6)(2016) 84-89.
[4] Z.-S. Dai, Q. Pan, G.-L. Chang, J.-G. Chen, Detection of Welding Defects in SMT Chip Pins Based on Machine Vision, Journal of Guangdong University of Technology 33(3)(2016) 65-69.
[5] W. Liang, L. Tao, G.-X. Zhang, Z.-H. Li, Welding defect detection method based on feature extraction and extreme searching, Journal of ShanDong University (Engineering Science) 44(3)(2014) 48-51.
[6] W. Luo, X.-J. Zou, J.-M. Chen, T.-G. Liang, H.-Y. Ding, Q.-X. Ni, Inspection System for PCB Pad of Mini LED Backlight Board Based on Machine Vision, Automation & Information Engineering 43(6)(2022) 20-26.
[7] Y. Liu, S. Wu, H.-H. Zhou, X.-J. Wu, L.-Y. Han, Research on optimization method based on K-means clustering algorithm, Information Technology 43(1)(2019) 66-70.
[8] Q. Liu, Y. Yan, Application of Sub-pixel Edge Extraction Method in the Positioning of Semiconductor Chips, Modern Information Technology 4(10)(2020) 55-57.
[9] J.-P. Zhao, H. Xu, Y.-Y. Dang, Research on bolt detection of railway passenger cars based on improved Faster R-CNN, China Safety Science Journal 31(7)(2021) 82-89.